

Evaluation of Image Pre-processing Techniques for Improved Rice Leaf Disease Detection

Ivyann Romijn H. Vergara and Mylah Rystie Anacleto

Abstract—This study presents a digital platform for automated rice disease detection, addressing the inefficiencies of traditional visual inspections. We evaluated various image pre-processing techniques—specifically, histogram equalization in L and V channels and contrast stretching with factors of 0.5 and 2—to enhance disease classification accuracy. The original image achieved the highest classification accuracy at 94.34%, followed by contrast stretching at a factor of 2 (92.24%) and factor of 0.5 (91.61%). Histogram equalization methods yielded lower accuracies (88.68% for L channel and 82.60% for V channel). These results reveal a complex relationship between image quality metrics and classification performance, indicating that while high Peak Signal-to-Noise Ratio (PSNR) and Structural Similarity Index (SSIM) suggest visual fidelity, they do not always correlate with improved disease detection. Future work will focus on integrating these findings into other Convolutional Neural Network models and developing a mobile app for real-time field detection.

Index Terms—image enhancement techniques, rice disease, CNN, histogram equalization, contrast stretching

I. INTRODUCTION

A. Background of the Study

The Philippines stands as one of the prominent consumers of rice in Asia and globally. Rice holds significant importance as a staple food and agricultural crop for Filipinos, constituting 37% of their daily diet and providing livelihood to 2.5 million households [1] [2]. As reported by the Philippine Statistics Authority, a total of 19.76 metric tons of palay were cultivated in 2022, with an average yield of 4.8 tons/ha - specifically 3.34 tons/ha in irrigated areas and 1.46 tons/ha in rainfed rice regions [3]. Given its status as a major rice-consuming nation across Asia and worldwide, the Philippines has long been striving towards achieving self-sufficiency in rice production while enhancing competitiveness against other nations. Efforts have been directed at minimizing yield losses resulting from environmental factors such as climate change (abiotic stresses) or biological factors like pests (biotic stresses).

Pest and disease damage significantly contributes to crop losses worldwide, with pathogen infections, animals, and weeds leading to yield reductions of 20% to 40% in agricultural production [4]. Globally, rice experiences a 30% yield loss due to various factors including diseases like rice tungro, bacterial leaf blight, rice blast, and sheath blight [5]. In the Philippines's Cagayan Valley region alone in 2022 at least 602 hectares were affected by rice blast across

Presented to the Faculty of the Institute of Computer Science, University of the Philippines Los Baños in partial fulfillment of the requirements for the Degree of Bachelor of Science in Computer Science

multiple localities such as Isabel, Quirino, and Cagayan which posed a threat to the country's rice production [6]. Disease management strategies emphasize prevention through proper detection techniques while employing good cultural practices that include high-quality seed planting methods along with effective water management and fertilizer application systems coupled with maintaining field sanitation standards [7]. Early disease detection in crops is the most crucial factor in minimizing yield losses from biotic stresses. By timely identifying and diagnosing diseases such as rice blast, bacterial leaf blight, and other fungal diseases, farmers can take proactive measures to prevent the spread of the diseases and minimize their impact on rice production [8] [9].

Traditional methods of identifying rice diseases rely on visual assessments by experienced farmers or trained inspectors, which are time-consuming and require specialized knowledge [8]. While biochemical technologies offer more precise detection, they are costly and not practical for most farmers. The emergence of nondestructive detection technologies like near-infrared spectroscopy [10], nuclear magnetic resonance spectroscopy [11], Fourier-transform infrared spectroscopy [12], and X-ray imaging [13] [14] has led to new ways of identifying rice seed variety and vigor. Advancements in computer and electronic technologies have also significantly improved image analysis techniques through machine learning and deep learning [15] [16], providing multidimensional information from rice crop images including color data, near-infrared spectra, three-dimensional representations as well as thermal radiation [17]. ML and DL have proven effective in plant disease detection through images compared to traditional methods with promising applications in the realm of rice disease identification [18] [19].

Machine learning and deep learning models have extensively investigated the effectiveness of various techniques such as k-means clustering, naive Bayes, feed-forward neural network, support vector machine, k-nearest neighbor classifier, fuzzy logic, genetic algorithm, artificial neural network, and convolutional neural network when using rice images for disease detection [20] [21] [22]. However, there is a noticeable lack of emphasis on assessing preprocessing techniques.

Preprocessing plays a crucial role in data preparation and can significantly influence the performance and accuracy of ML and DL models. Tasks such as image enhancement, normalization, and feature extraction are important aspects of preprocessing that can improve input data quality, enhance model efficiency, and increase overall disease detection accuracy. Therefore, it is essential to evaluate preprocessing techniques to ensure that input data is appropriately pro-

cessed and optimized for the specific requirements of ML and DL algorithms, ultimately leading to more reliable disease detection models in applications related to rice diseases [20] [21].

B. Significance of the Study

The study aimed to improve the accuracy of rice leaf disease detection through image enhancement techniques. By comparing and evaluating different image enhancement methods, the most effective ones for improving image quality were identified, enhancing disease visibility and contributing to significantly improved detection accuracy, leading to earlier diagnosis and better treatment outcomes.

Furthermore, image quality metrics like Peak Signal-to-Noise Ratio (PSNR), Normalized Root Mean Squared Error (NRMSE), and Structural Similarity Index (SSIM) were evaluated. These metrics provide valuable insights into different aspects of image quality.

Beyond refining image enhancement techniques, the research aimed to translate these advancements into a tangible tool with web platform. This tool had the potential to revolutionize early diagnosis of rice diseases, especially in regions where access to specialized agricultural expertise and advanced imaging technologies remained limited.

By optimizing image pre-processing techniques, the study contributed to the advancement of AI-based systems for rice disease detection. This paved the way for more accurate and automated diagnosis, potentially leading to improved agricultural practices and reduced reliance on subjective visual inspections.

Ultimately, the goal of the study was to improve the accuracy and accessibility of rice leaf disease detection. This had the potential to significantly enhance crop management, increase yield, and reduce agricultural losses [8].

This research investigated the most reliable pre-processing technique to complement a CNN-based approach for rice leaf disease detection. By exploring the potential of image enhancement alongside AI algorithms, the study aimed to revolutionize rice disease detection. The research addressed common challenges associated with image quality and developed a user-friendly web application for rice disease detection, where early diagnosis and efficient management of rice diseases become more accessible.

C. Statement of the Problem

Advancements in the detection of crop diseases have progressed, but the early and precise identification still presents a difficulty. This is due to the absence of distinct visual symptoms of rice diseases. Although ML and DL techniques are beneficial, there is limited research on pre-processing methods. Furthermore, existing approaches frequently depend on farmers' visual inspections, which are subjective and susceptible to inconsistencies.

D. Objectives of the Study

The objective of this study was to develop a digital platform for automated identification of rice diseases. The research also

assessed various approaches to enhance the quality of images depicting rice diseases, with the goal of improving detection precision validated by statistical analyses. It primarily concentrated on leaf-related illnesses including bacterial blight, brown spot, rice blast, leaf scald, and narrow brown spot.

E. Scope and Limitations

The research focused on various rice leaf diseases, including bacterial blight, brown spot, rice blast, leaf scald, and narrow brown spot.

This study investigated the performance of various pre-processing techniques, including histogram equalization in the L channel of the LAB color space and the V channel of the HSV color space, as well as contrast stretching with factors of 0.5 and 2. These techniques were evaluated using statistical metrics including peak signal to noise ratio, normalized root mean square error, and structural similarity index.

The research was limited by the available devices, namely an 11th Gen Intel(R) Core(TM) i5-1135G7 @ 2.40GHz Acer Laptop. If more processing power was needed, a 2 TB RAM Server available in CINTERLABS in the Physical Sciences Building at UPLB could have been used for shared use by its various beneficiaries.

II. RELATED LITERATURE

Artificial intelligence (AI) and machine learning (ML) are revolutionizing agriculture, offering immense promise for improving crop yields and sustainability. Its deep learning expertise enables automation and enhancement of crop monitoring, disease detection, and precision farming. ML models surpass human experts in predicting crop health, soil conditions, and pest infestations, showcasing potential beyond agriculture for improving food security and environmental sustainability across ecosystems. Further development and implementation of AI-ML are crucial to optimize agricultural practices and ensure global food security [23].

A thorough examination of AI and ML techniques for detecting rice diseases is presented in [24]. The review evaluates a range of AI, ML, and deep learning approaches for identifying rice diseases, highlighting the significance of the rice plant on a global scale. It indicates that CNN achieves superior accuracy in detecting rice leaf diseases surpassing other models, possibly due to its ability to capture intricate information at deeper layers. For example, lower-level features such as edges are identified in the initial layers, followed by simpler shapes in subsequent layers, culminating with higher-level characteristics.

A study [25] assessed the performance of various deep learning architectures (AlexNet, VGG16, VGG19, GoogleNet, ResNet18, ResNet50, ResNet101, InceptionV3, InceptionResNetV2, DenseNet201, Xception) in extracting features for classifying rice diseases using SVM. Transfer learning was then applied to these models to identify rice diseases. Performance analysis included evaluation of transfer learning and feature extraction methods as well as small CNN models (MobileNetv2 and Shufflenet) using both approaches. The superior model was selected based on statistical analysis with

Tukey's honest significance test showing that Resnet50 plus SVM achieved an F1 score of 0.9838 with a training time of 69 seconds in feature extraction approach; no significant difference among the CNN models observed in the transfer learning approach; Mobile-netv2's deep feature plus SVM attained an F1 score of 0.9796 with a training time of 48 seconds, making it comparable to resnet50 plus SVM.

Another study [26] investigated automated diagnosis of rice blast disease using pre-trained models such as Inception V3, VGG16, VGG19, and ResNet50. The researchers made use of a publicly available dataset comprising 2,000 images. These images were categorized into approximately 1,200 pictures of rice leaves with blast disease and 800 images of healthy leaves. Among the various models tested in the study, a customized version of ResNet50 achieved the highest accuracy at 99.75% with a minimal loss rate (error rate) of 0.33. Additionally, Inception V3, VGG16, and VGG19 also demonstrated strong performance levels with accuracies reaching 98.16%, 98.47%, and 98.56% respectively. The reliability of ResNet50's performance was confirmed through additional measures whereby it showed a validation accuracy of 99.69%, demonstrating its effectiveness on unseen data. Moreover, the model exhibited high precision (99.50%), F1-score (99.70%), and AUC (Area Under the Curve) of 99.83%, indicating its ability to accurately identify both healthy and diseased leaves with minimal false positives and negatives.

However, there is a noticeable lack of emphasis on evaluating pre-processing techniques in these studies. Preprocessing is a crucial step in data preparation that can significantly impact the performance and accuracy of machine learning and deep learning models [27]. It involves transforming an input image and conducting various processes to either enhance the image or extract important data from it. It is a form of signal processing where the input is an image and the output may be either an enhanced image or characteristics associated with that image [28]. Image pre-processing encompasses noise reduction, color conversion, and detail enhancement techniques that are essential for improving the accuracy of disease detection. Thus, a review article [29] examined the widespread application of image processing in different approaches to diagnosing plant diseases, aiding experts in determining appropriate treatments. The article highlighted that diagnostic methods utilizing image pre-processing often achieve accuracy rates exceeding 90%.

Outlined in Table 1 summarizes the findings from various studies that have applied image pre-processing techniques for plant disease detection.

TABLE I
IMAGE PRE-PROCESSING TECHNIQUES IN RELATED LITERATURE

| Reference | Data | Method |
|-----------|-----------------------------|------------------------------------|
| [30] | Wheat Rust | Histogram Equalization |
| [31] | Lemon Grass | Histogram Equalization |
| [32] | Various plant leaf diseases | Image Sharpening and Median Filter |
| [33] | Maize plant | CLAHE and Color Conversion |
| [34] | Tobacco | Contrast Stretching |

[30] utilized Histogram Equalization on the R, G, and B planes as well as the Hue-Saturation-Value color space model for contrast enhancement. The authors compared the original histogram with the equalized histogram using image quality improvement metrics like MSE and PSNR. Consequently, it can be concluded that employing histogram equalization techniques is an effective method to improve image quality. Additionally, the traditional histogram equalization technique is employed to enhance and improve the images of lemon grass [31]. The efficiency of the system is computed using MatLab. The simulation results indicate that, despite being a conventional method, Histogram Equalization has the capability to effectively improve images and reveal hidden details present in each image.

While histogram equalization offers a valuable approach for contrast enhancement, other pre-processing techniques can also be beneficial. One study investigated the use of image sharpening and median filtering for noise reduction in plant disease detection. PSNR (Peak Signal-to-Noise Ratio) served as the evaluation metric, with higher values indicating improved image quality. The results concluded that images pre-processed with sharpening and median filtering yielded better identification of plant leaf diseases compared to unprocessed images [32].

Additionally, Contrast Limiting Adaptive Histogram Equalization (CLAHE) is another pre-processing technique that has shown promising results in plant disease detection, achieving a maximum accuracy of 99.9978% using CNN [33]. Furthermore, contrast stretching transformation has been also used in conjunction with neural networks for plant disease classification. For instance, a study successfully classified seedling diseases, such as frog eye spot on tobacco leaves, using a neural network [34].

On top of preprocessing methods, a research study [35] investigated and evaluated Grayscale and RGB images using image processing techniques including preprocessing, segmentation, clustering for the detection of leaf diseases. Color was found to be a crucial feature in identifying disease severity when detecting infected leaves. The use of RGB images resulted in clearer and less noisy images that are more suitable for detecting infected leaves than Grayscale images.

III. MATERIALS AND METHODS

A. Data Set

An open-source dataset from Roboflow Universe entitled "Rice Leaf Disease detection obj Computer Vision Project" [36] was used in this project. The dataset encompasses a variety of rice leaf images categorized into six classes as shown on the table below:

Figure 1 shows sample images from the classes.

B. Image Preprocessing

1) *Histogram Equalization*: Histogram equalization (HE) is an image processing technique that enhances the overall contrast of images by redistributing pixel values. It is particularly effective when the image has a narrow range of intensity values, as it aims to make the histogram more evenly

| Name | No. of Images |
|-----------------------|---------------|
| Healthy | 434 |
| Bacterial Leaf Blight | 361 |
| Brown Spot | 394 |
| Leaf Blast | 358 |
| Leaf Scald | 358 |
| Narrow Brown Spot | 408 |
| TOTAL | 2313 |

TABLE II

NUMBER OF IMAGES IN THE RICE LEAF DISEASE DATASET

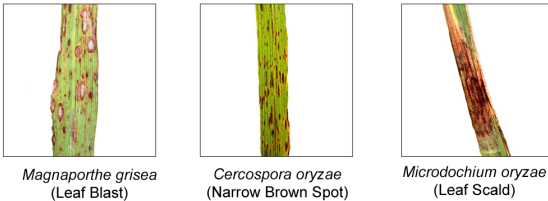
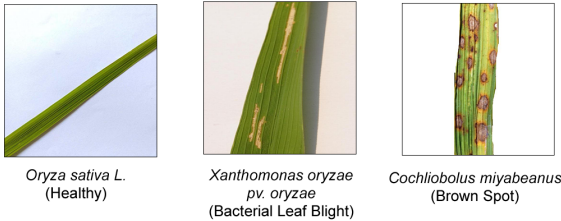


Fig. 1. Sample images from each rice leaf disease class

distributed across the entire intensity axis. This process results in a non-linear extension of the image, improving the visual quality and making it easier to analyze [37]. In this study, there are two types of histogram equalization; Histogram Equalization in LAB color space and in HSV color space. The image is first converted to the corresponding color space and applied Histogram Equalization in L channel and V channel, respectively and converted back to RGB color space. Figure 2 and Figure 3 visually demonstrates the transformation of the pixel intensity distribution after equalization in a sample image .

2) *Contrast Stretching*: Contrast stretching can significantly improve the visibility of rice leaf diseases by enhancing the contrast between healthy and diseased areas. This technique works by manipulating the image histogram. The histogram represents the distribution of pixel intensities in the image. Contrast stretching expands this distribution, essentially stretching the range of intensity values across the available spectrum which can be shown in Figure 3 and Figure 4. This makes subtle differences between healthy and infected tissues more prominent. By increasing the separability of these structures in the histogram, the overall image quality is improved. This translates to clearer distinctions between healthy and diseased leaf regions, aiding in accurate disease identification and segmentation. This improved clarity is crucial for precisely

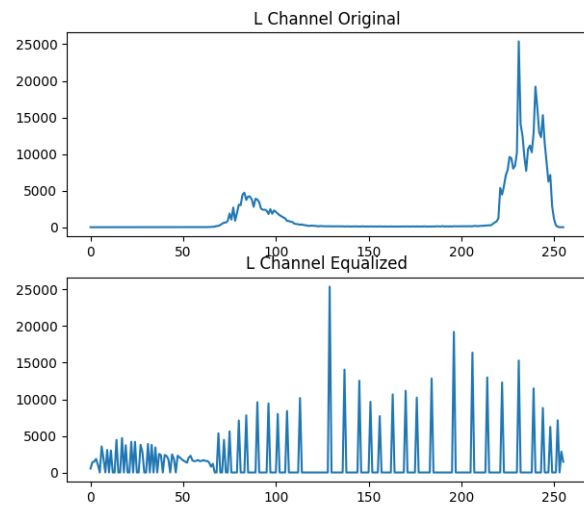


Fig. 2. Pixel Intensity Distribution in L channel

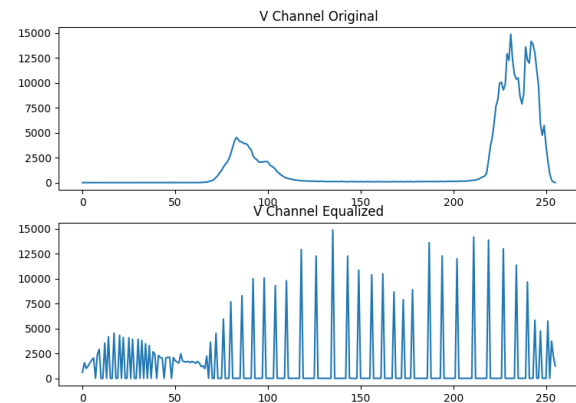


Fig. 3. Pixel Intensity Distribution in V channel

delineating the boundaries, shapes, and other characteristics of rice leaf lesions, which is critical for accurate segmentation and disease diagnosis [38]. We used contrast stretching with factor set at 0.5 delivered high image contrast while using a factor value of 2 resulted in low image contrast.

The images below shows the results before and after applying pre-processing techniques on some classes.

C. Image Augmentation

To enhance the generalization capability of our image model, we implemented a image augmentation [39]. This process involved artificially modifying each image in the training dataset. We achieved this by applying various techniques. Images were randomly rotated within a range of -20 to +20 degrees, introducing variations in perspective to simulate real-world rotations. To account for slight camera movements, images were also randomly shifted horizontally and vertically by up to 20% of their original dimensions. Additionally,

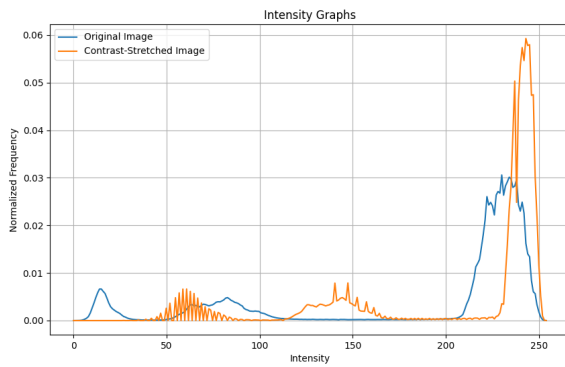


Fig. 4. Intensity Graph of Contrast Stretching (0.5)

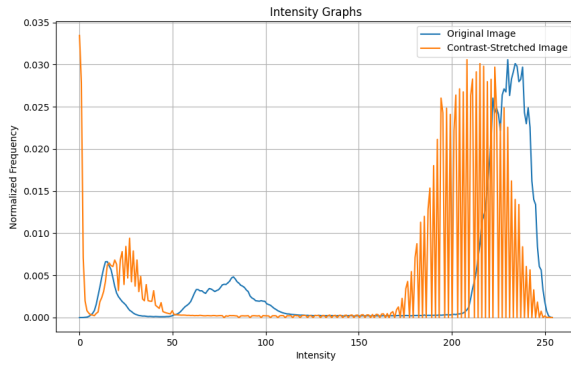


Fig. 5. Intensity Graph of Contrast Stretching (2.0)

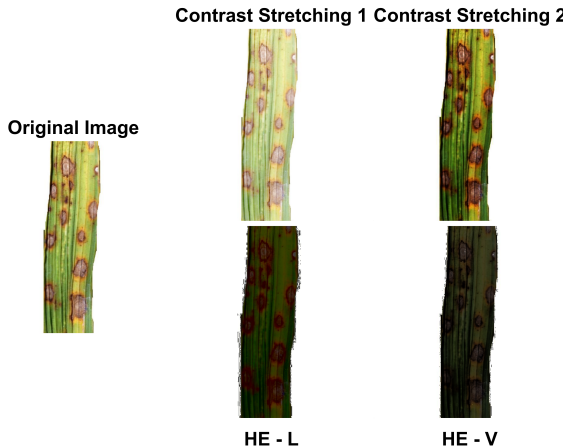


Fig. 6. (a) Leaf with Brown Spot disease, (b) After contrast stretching with power of 0.5, (c) After contrast stretching with power of 2, (d) After Histogram Equalization in L channel, (e) After Histogram Equalization in V channel

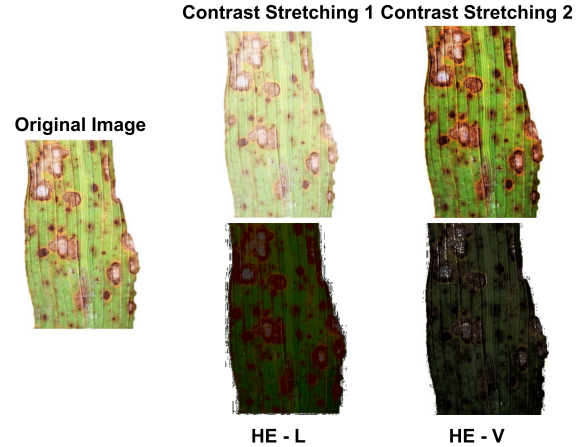


Fig. 7. (a) Leaf with Leaf Blast disease, (b) After contrast stretching with power of 0.5, (c) After contrast stretching with power of 2, (d) After Histogram Equalization in L channel, (e) After Histogram Equalization in V channel

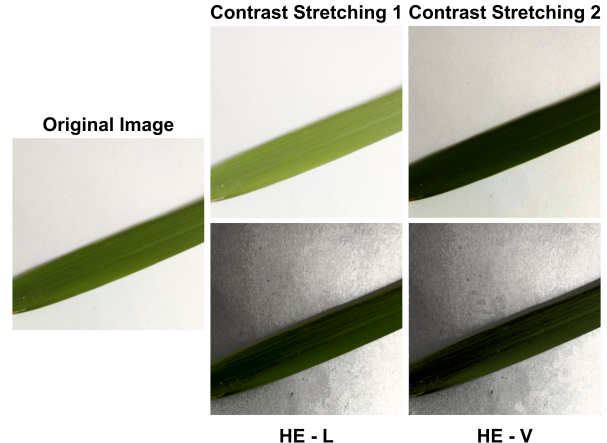


Fig. 8. (a) Healthy Leaf, (b) After contrast stretching with power of 0.5, (c) After contrast stretching with power of 2, (d) After Histogram Equalization in L channel, (e) After Histogram Equalization in V channel

zooming was applied by a random factor between 0.8 and 1.2, mimicking the effects of zooming a camera lens. To simulate shearing effects, images were also randomly sheared horizontally by a factor between -0.2 and 0.2. Finally, to account for objects appearing from different directions, each image had a chance of being flipped horizontally and vertically.

D. Model Training

We trained our models using ConvXT, a convolutional neural network (CNN) development tool from CINTERLABS created by Mojari [40]. ConvXT allows us to easily configure training parameters like epochs, batch size, and validation steps. In this study, we used a training regimen of 100 epochs, a batch size of 16, 50 steps per epoch, and 15 validation steps. ConvXT also provides visualizations of the training process, including accuracy and loss graphs.

Furthermore, ConvXT incorporates transfer learning, a technique that leverages pre-trained CNN models (like ResNet-50, InceptionV3, and VGG16 included in Keras) as a starting point

for building new models. In this case, we employed ResNet-50, aligning with similar research.

E. Quality Metrics

1) *Peak Signal-to-Noise Ratio (PSNR)*: The Peak Signal-to-Noise Ratio assesses the quality variation between two images in decibels, examining the correlation between the maximum signal value and the impact of noise on enhanced image signals. It is frequently employed to evaluate the quality of an output image in comparison to the original. A higher PSNR value signifies better output image quality, with its calculation derived from Mean Squared Error as depicted in Equation 1 [41]. In Python's scientific image processing library, Scikit-image, the PSNR calculation can be conveniently performed using the `skimage.metrics.peak_signal_noise_ratio` function. [42]

$$PSNR = 20\log_{10}\left(\frac{MAX_f}{\sqrt{MSE}}\right) \quad (1)$$

Typical PSNR values for lossy image and video compression fall within the range of 30 to 50 dB, with higher values indicating better quality. It is generally considered that values exceeding 40 dB are excellent, while those below 20 dB are deemed unacceptable [43].

2) *Normalize Root Mean-Squared Error (NRMSE)*: The NRMSE is a metric that considers the magnitude of the errors between two sets of data. It is similar to the Root Mean Squared Error (RMSE), but it is normalized by the maximum and minimum value of the data as shown on equation 2 denoted by Y_{max} and Y_{min} . This normalization makes the NRMSE independent of the scale of the data, allowing for easier comparison between images with different intensity ranges [44]. In the context of image processing, a lower NRMSE value indicates a better match between the original and the processed image [45]. In this specific case, the NRMSE can be conveniently computed using the `skimage.metrics.normalized_root_mse` function from Scikit-image [42].

$$NRMSE = \frac{1}{Y_{max} - Y_{min}} \sqrt{\frac{\sum_{i=1}^N (Y_i - \hat{Y}_i)^2}{N}} \quad (2)$$

NRMSE values equal to or below 0.1 indicate excellent reconstruction with minimal pixel intensity variations. As NRMSE rises between 0.1 and 0.2, the quality of reconstruction becomes satisfactory, although there may be some noticeable distortion present. If the NRMSE exceeds 0.2, the reconstruction is likely to have significant intensity variations and could appear visually distorted. [46]

3) *Structural Similarity Index (SSIM)*: This metric assesses the similarity in underlying structural information between the pre-processed and enhanced rice leaf images. A higher or closer to 1 SSIM value indicates that the enhancement process effectively retains the original details of the rice leaf, such as vein structures and textures, while simultaneously highlighting potential disease signatures. This

preservation of structural details is crucial for accurate disease diagnosis and monitoring of disease progression in rice crops [47]. It can be conveniently computed using the `skimage.metrics.structural_similarity` function from Scikit-image [42]. Equation 3 shows the formula for SSIM where, $I(x, y)$ being an image, μ_x being the average value for x or luminance x , μ_y being the average value for y or luminance y , σ_y the contrast value for y , σ_x for the contrast value of x , c_1 and c_2 being the two variables used to stabilize the division if the divisor is 0.

$$SSIM(x, y) = \frac{(2\mu_x\mu_y + c_1)(2\sigma_{xy} + c_2)}{(\mu_x^2 + \mu_y^2 + c_1)(\sigma_x^2 + \sigma_y^2 + c_2)} \quad (3)$$

When the SSIM is greater than 0.9, it typically signifies a high level of structural similarity, making it suitable for tasks that demand precise representation. If the SSIM falls between 0.8 and 0.9, this indicates favorable structural similarity which is generally acceptable for various purposes. However, if the SSIM is less than or equal to 0.8, then the structural similarity diminishes and there may be noticeable imperfections or distortions in the reconstructed image [48].

F. Model Performance

The model's performance was assessed using ConvXT, which evaluates its effectiveness on the test data by producing a classification report. This comprehensive report includes various metrics such as precision, recall, F1-score, support, overall accuracy, macro average and weighted average of the model.

G. Rice Leaf Disease Detection Interface

The web application was built using HTML 5 and CSS 3 for the front-end user interface, and the Flask micro-framework served as the back-end development tool. This combination aimed to provide an interactive environment for screening rice plants affected by various leaf diseases. The web application starts by allowing users to select an image of a rice leaf from their computer. Once an image is chosen, a confirmation message appears, and an "Upload and Classify" button becomes active. Clicking this button triggers the process. The application retrieves the image and applies the pre-processing techniques to prepare it for analysis. Then, the image is fed into multiple trained models, each using different processing techniques to identify rice leaf diseases. Each model analyzes the image and predicts the disease (if any) along with a confidence score indicating the accuracy of the prediction. The user interface displays both the original and processed image (depending on the technique) alongside the detected disease and its corresponding accuracy score for each technique used. Additionally, an optional "Show Details" button allows users to expand the results section and see more information about each classification, showing a breakdown of the confidence score for each possible disease, and any relevant intermediate results generated during the analysis.

IV. RESULTS AND DISCUSSION

The results from the implementation of pre-processing techniques for the detection and classification of rice leaf diseases are reported in this section.

A. Image Enhancement

1) *Quality Metrics:* The metrics presented in Table III is used to assess the quality of the obtained images.

TABLE III
QUALITY METRICS FOR IMAGE ENHANCEMENT TECHNIQUES

| Pre-processing Technique | Class | PSNR | NRMSE | SSIM |
|-----------------------------|-------------------|----------------|---------------|---------------|
| Histogram Equalization | Healthy | 9.8553 | 0.3270 | 0.4198 |
| | brown spot | 11.06970 | 0.2932 | 0.6359 |
| | leaf blast | 11.2046 | 0.2973 | 0.5236 |
| | leaf blight | 14.2869 | 0.2025 | 0.7004 |
| | leaf scald | 14.5963 | 0.1921 | 0.8654 |
| | narrow brown spot | 14.5063 | 0.1921 | 0.8523 |
| | Mean | 12.5865 | 0.2507 | 0.6662 |
| Contrast Stretching 1 (0.5) | Healthy | 19.4101 | 0.1089 | 0.9343 |
| | brown spot | 20.2928 | 0.1009 | 0.9510 |
| | leaf blast | 20.1845 | 0.1084 | 0.9503 |
| | leaf blight | 19.3871 | 0.1120 | 0.9534 |
| | leaf scald | 24.3503 | 0.0632 | 0.9812 |
| | narrow brown spot | 22.5093 | 0.0765 | 0.9694 |
| | Mean | 21.0224 | 0.0950 | 0.9566 |
| Contrast Stretching 2 (2) | Healthy | 17.7859 | 0.1315 | 0.9343 |
| | brown spot | 18.6410 | 0.1238 | 0.9510 |
| | leaf blast | 18.0705 | 0.1410 | 0.9503 |
| | leaf blight | 17.1845 | 0.1441 | 0.9534 |
| | leaf scald | 23.5116 | 0.0693 | 0.9812 |
| | narrow brown spot | 22.1617 | 0.0795 | 0.9694 |
| | Mean | 19.5592 | 0.1149 | 0.9566 |

When evaluated using the PSNR metric, contrast stretching with a power of 0.5 (CS1) yielded the highest result at 21.0224, followed by contrast stretching with a power of 2 (CS2) at 19.5592. In comparison, both histogram equalization (HE-L and HE-V) resulted in the lowest score at 12.4422 and 12.6132, respectively. Examination of individual classes revealed that "leaf scald" consistently had the highest PSNR value across all techniques, while "healthy" and "leaf blight" had the two lowest values in contrast stretching. As for the two histogram equalization, it produced the classes the produced the lowest scores are healthy" and "brown spot". The majority of PSNR values fall outside the conventionally accepted range, with a threshold of approximately 20 dB. Notably, only CS1 and CS2, specifically for the leaf scald and narrow brown spot classes, achieved PSNR values that meet this established criterion.

Considering the NRMSE metric, CS1 produced results closest to the original image at 0.0950, while HE-V exhibited

greater disparity from the original image at 0.2527. However, when analyzing individual classes' NRSME values for CS2 contradicted those observed for PSNR; leaf blight and leaf blast exhibited higher NSMR values instead of healthy and leaf blight in but remained consistent in classifying leaf scald as best quality. Additionally, in HE, it produced the highest value in classes healthy and leaf blast which contrasts with the findings in PSNR of classes healthy and brown spot. In accordance with the established benchmarks for NRMSE values as outlined in the relevant literature, only CS1 and CS2 achieved satisfactory reconstruction quality. Furthermore, within the HE methods, solely the leaf scald and narrow brown spot categories met the criteria. The remaining HE classes exhibited NRMSE values exceeding the acceptable thresholds.

Based on the SSIM scores of various methods, it was observed that both forms of contrast stretching yielded similar results. This similarity can be attributed to the fact that contrast stretching works by adjusting the distribution of intensity values in an image, essentially remapping existing intensity values to a new range and either expanding or compressing the contrast. Notably, this process does not introduce entirely new intensity values beyond the original image's range [38]. SSIM aligns with the individual disease performances observed in PSNR for leaf scald, indicating the closest resemblance to the original image. However, in both HE, instead of identifying healthy and brown spot as the worst, the SSIM result indicated healthy and leaf blast as having the lowest similarity. Conversely, contrast stretching showed that instead of identifying healthy and leaf blight, the SSIM results displayed healthy and leaf blast. The SSIM findings are comparable to NRMSE, CS1 and CS2 both demonstrated a high degree of structural similarity. However, only the leaf scald and narrow brown spot categories met the acceptable criteria within the HE method.

TABLE IV
SUMMARY OF THE QUALITY METRICS

| Method | PSNR | | NRMSE | SSIM |
|--------|-------|----------------------|-------------------------|---------------------|
| HE-L | Best | Leaf scald | Leaf scald | Leaf scald |
| | Worst | Healthy, brown | Healthy, leaf blast | Healthy, leaf blast |
| HE-V | Best | Leaf scald | Leaf scald | Leaf scald |
| | Worst | Healthy, brown | Healthy, leaf blast | Healthy, leaf blast |
| CS1 | Best | Leaf scald | Leaf scald | Leaf scald |
| | Worst | Healthy, leaf blight | Healthy, leaf blight | Leaf blast |
| CS2 | Best | Leaf scald | Leaf scald | Leaf scald |
| | Worst | Healthy, leaf blight | Leaf blast, leaf blight | Leaf blast |

Considering all the metrics, contrast stretching, particularly with a power of 0.5 (CS1), achieved a good performance in preserving image quality of the rice leaf. This is because higher PSNR indicates better signal-to-noise ratio, lower NRMSE signifies less reconstruction error, and higher SSIM reflects greater structural similarity to the original image. In this analysis, CS1 achieved the highest PSNR and SSIM values, while also demonstrating NRMSE, suggesting it effectively retains both image quality and structural details.

While these metrics provide valuable insights into image quality, it's crucial to evaluate their impact on the actual

classification performance. Ideally, the chosen pre-processing technique (like CS1 based on our analysis) should lead to a confusion matrix in section C that demonstrates high diagonal values compared to HE and CS2.

B. Model Performance

The figures (Fig.9-Fig.13) illustrate the accuracy and loss during model training on images. The x-axis indicates the epochs, which denotes the number of times the entire dataset is fed through the model in training. The top graph's y-axis represents accuracy, while the bottom graph's y axis depicts loss.

Generally, as the number of epochs increases, the training accuracy increases and the training loss decreases. This indicates that the model is learning to better classify the images. Moreover, the validation accuracy and loss curves should follow a similar trend to the training accuracy and loss curves. If the validation accuracy starts to diverge from the training accuracy, it could be a sign of overfitting. Overfitting is when the model learns the training data too well, but it is not able to generalize well to unseen data [49].

In Fig.9-Fig.13 the training accuracy is relatively high and the training loss is relatively low, which suggests that the models are performing well.

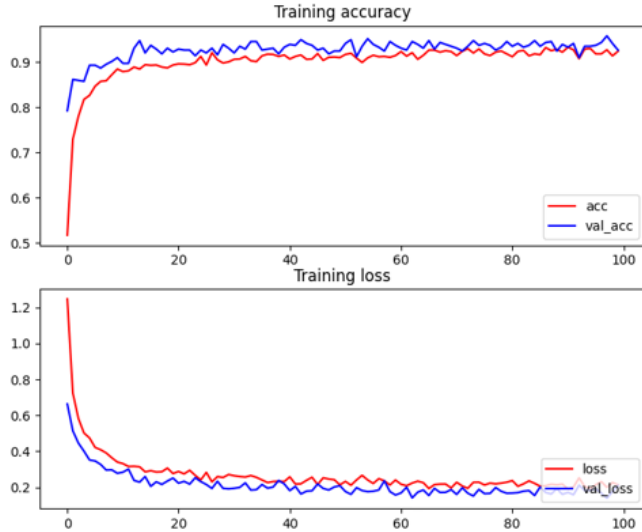


Fig. 9. History graph for the accuracy and loss of the model on raw images

C. Image Classification Metrics

A confusion matrix is a powerful tool for analyzing the performance of a model classifying different rice leaf diseases. Each row represents a specific disease, and each column shows the model's predictions for those images. Ideally, high values on the diagonal (True Positives and True Negatives) indicate the model accurately identified healthy and diseased plants. However, off-diagonal cells reveal misclassifications and can pinpoint which diseases are more difficult for the model to distinguish [50]. To gain deeper insights into the model's

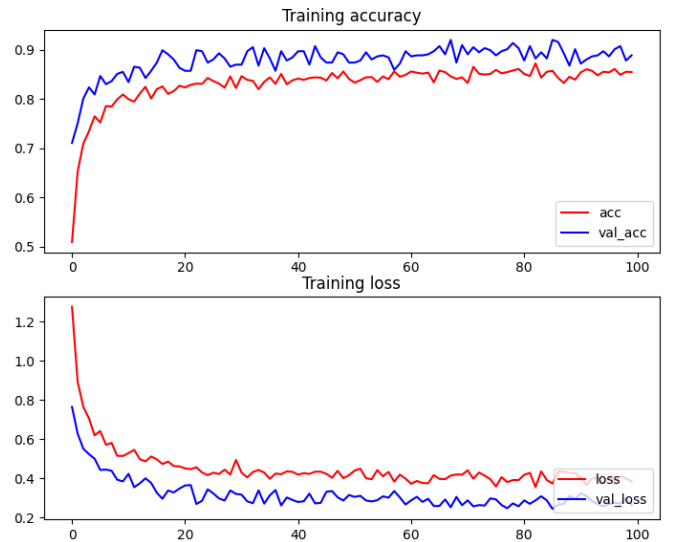


Fig. 10. History graph for the accuracy and loss of the model on HE L-Processed Images

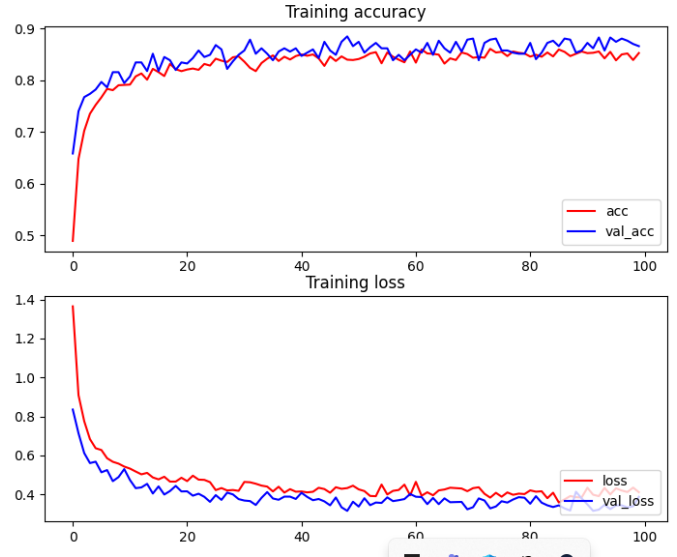


Fig. 11. History graph for the accuracy and loss of the model on HE V-Processed Images

performance, we analyze the individual cells of the confusion matrix:

- **True Positive:** This refers to the number of images where the model correctly identified a specific rice disease. For instance, the value in the "blast disease" row and "blast disease" column would represent the count of images with confirmed blast disease that were accurately classified by the model. In essence, these are successful disease detections.
- **True Negative:** This indicates the number of images where the model correctly classified a healthy rice plant (no disease). In the confusion matrix, this would be the cell where both the actual class label (row) and the model's predicted class (column) are "Healthy." These

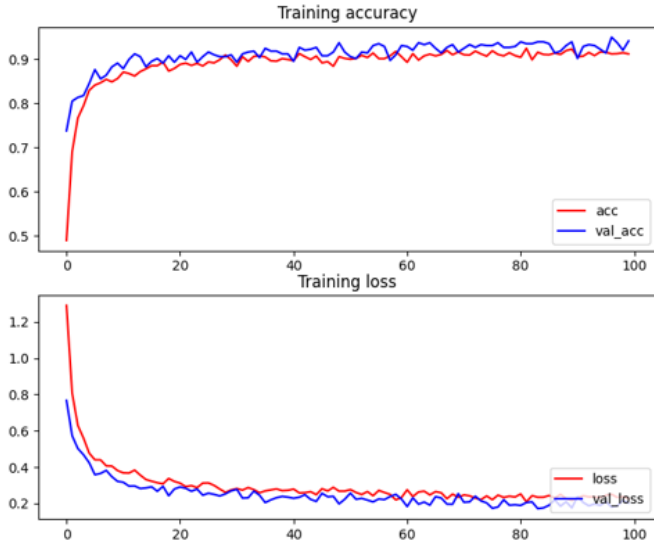


Fig. 12. History graph for the accuracy and loss of the model on CS-Processed Image (Power of 0.5)

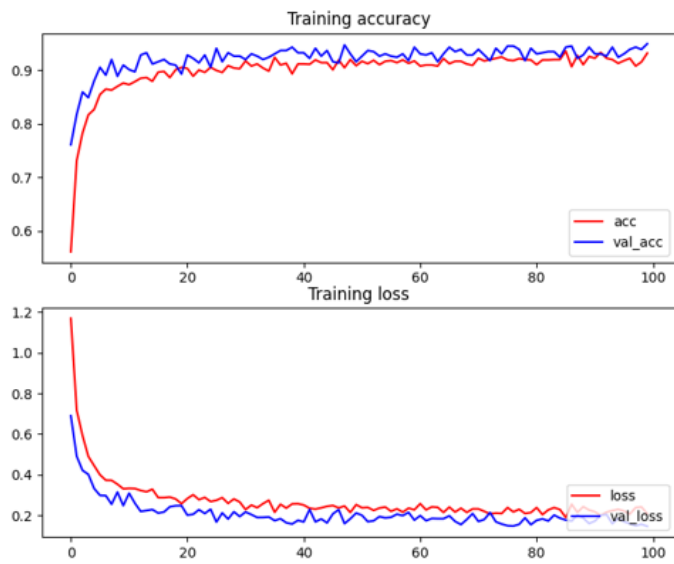


Fig. 13. History graph for the accuracy and loss of the model on CS-Processed Image (Power of 2)

represent accurate identifications of healthy plants

- False Positive: This denotes the number of images where the model incorrectly identified a disease. Continuing the example, if an image shows no signs of any disease but is predicted by the model to have "bacterial leaf blight," it would be considered a false positive. These represent misclassifications of healthy plants as diseased.
- False Negative: This describes the instances when the model failed to detect a certain disease. For example, if an image displays "sheath blight" but gets misclassified as being healthy by the model, it constitutes a false negative. These represent missed disease detections.

Figure 14 depicts the confusion matrix of model on raw

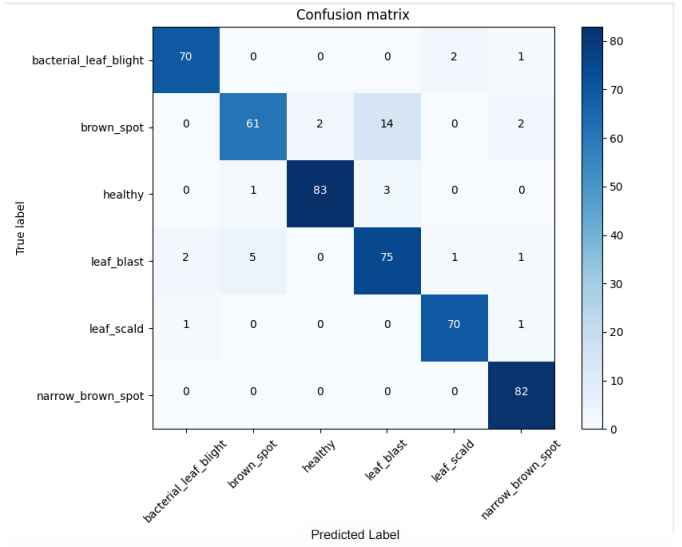


Fig. 14. Confusion Matrix of Model on Raw Images

images, indicating that the model struggles the most when categorizing brown spots. Out of 79 rice leaves, only 61 were accurately classified. There is a tendency to misclassify it as leaf blast instead of its true label brown spot. Regardless, all other classes were correctly classified with no more than 5 misclassifications each.

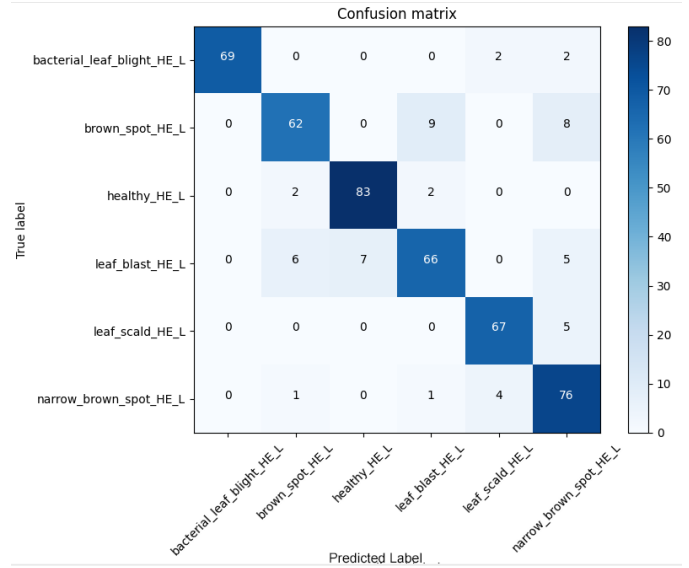


Fig. 15. Confusion Matrix of the model on HE L-Processed Image

Consistently with Figure 14, Figure 15 demonstrates a misclassification of brown spots as leaf blast.

In figure 16, a significant number of false negative are evident, where the model identifies it as healthy but its true label is leaf blast.

In figure 17, the misclassification of the brown spot as leaf blast significantly reduced. However, it struggles to differentiate between leaf blast and brown spot, misclassifying 13 leaf blast instances as brown spot.

The confusion matrix shown in figure 18 also reveals a high

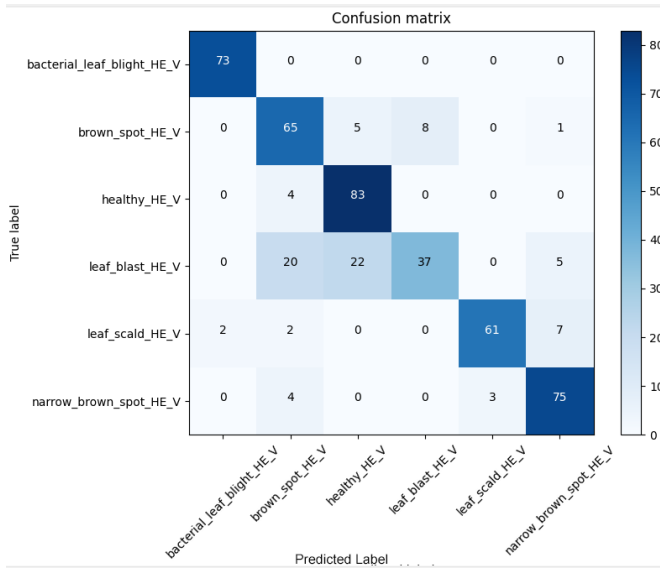


Fig. 16. Confusion Matrix of the model on HE V-Processed Image

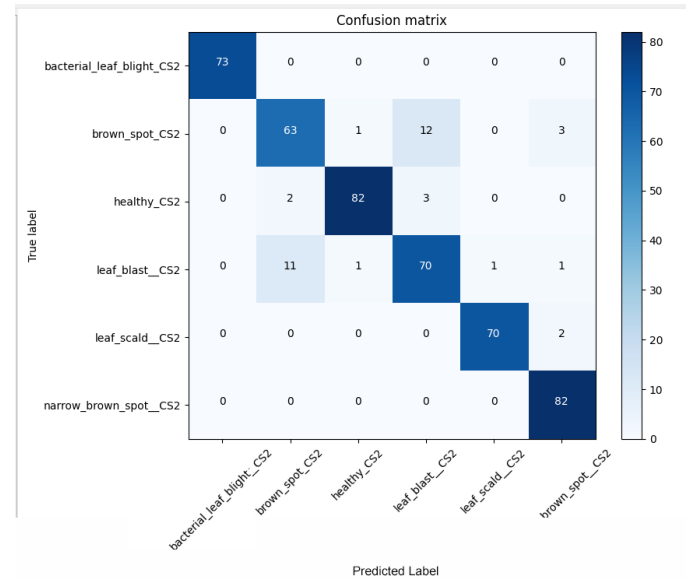


Fig. 18. Confusion Matrix of the model on CS-Processed Image (2)

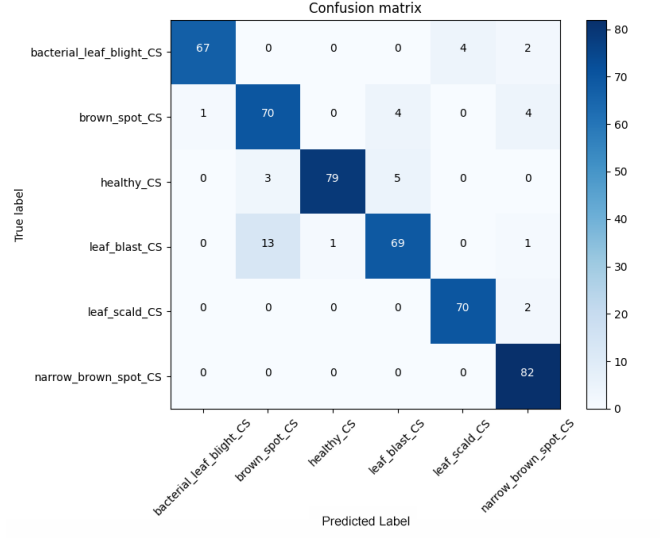


Fig. 17. Confusion Matrix of the model on CS-Processed Image (0.5)

rate of misclassifications between brown spot and leaf blast.

The figures 6-8 depict sample visuals of brown spot, leaf blast, and healthy rice leaves, both before and after applying preprocessing techniques. This provides a visual illustration of the most frequently misclassified diseases.

Table V shows the classification report for two image enhancement techniques, Histogram Equalization in L channel (HE-L), Histogram Equalization in V channel (HE-V), and Contrast Stretching (CS1 and CS2), applied to images of rice leaves with different diseases alongside the original image. The metrics used are precision, recall, F1 score, and accuracy.

In the context of rice disease detection, precision refers to the proportion of rice plants correctly identified as having a specific disease out of all the plants flagged as having that disease.

$$\text{Precision} = \frac{\text{TruePositive}(TP)}{\text{TruePositive}(TP) + \text{FalsePositive}(FP)} \quad (4)$$

Recall measures tells us how many of the leaves with a specific disease were correctly identified by the image enhancement technique. Mathematically:

$$\text{Recall} = \frac{\text{TruePositive}(TP)}{\text{TruePositive}(TP) + \text{FalseNegative}(FN)} \quad (5)$$

A model might have high precision but miss some actual cases (low recall) or vice versa. The F1 score tries to find a balance between these two metrics. Thus, the F1 score is the harmonic mean of precision and recall. Calculates as Equation 6.

$$\text{F1Score} = 2 * \left(\frac{\text{Precision} * \text{Recall}}{\text{Precision} + \text{Recall}} \right) \quad (6)$$

The table shows that CS2 seems to perform better than CS1 and both HE for most diseases. For example, for bacterial leaf blight, CS2 has a precision, recall and F1-score of 1.0000 , while CS1 has a precision of 0.9853 and a recall of 0.9178 and HE has a precision of 0.9114 and recall of 0.9863. This means that CS2 correctly identified all the leaves with bacterial leaf blight (precision), and 100% of the leaves actually having bacterial leaf blight were identified correctly (recall).

While CS2 demonstrates superior performance in detecting bacterial leaf blight, the original image still exhibits a higher

TABLE V
CLASSIFICATION REPORT OF MODELS

| Model | Class | Precision | Recall | F1-Score |
|--------------------------------|------------------------------|---------------|---------------|---------------|
| Orginal Image | bacterial_leaf_blight | 1.0000 | 0.9726 | 0.9861 |
| | brown_spot | 0.8846 | 0.8734 | 0.8790 |
| | healthy | 0.9880 | 0.9425 | 0.9647 |
| | leaf_blast | 0.8929 | 0.8929 | 0.8929 |
| | leaf_scald | 0.9726 | 0.9861 | 0.9793 |
| | narrow_brown_spot | 0.9318 | 1.0000 | 0.9647 |
| | accuracy | 0.9434 | 0.9434 | 0.9434 |
| | macro avg | 0.9450 | 0.9446 | 0.9444 |
| HE processed Image (L channel) | weighted avg | 0.9440 | 0.9434 | 0.9433 |
| | bacterial_leaf_blight_HE0D00 | 0.9452 | 0.9718 | |
| | brown_spot_HE_L | 0.8732 | 0.7848 | 0.8267 |
| | healthy_HE_L | 0.9222 | 0.9540 | 0.9379 |
| | leaf_blast_HE_L | 0.8462 | 0.7857 | 0.8148 |
| | leaf_scald_HE_L | 0.9178 | 0.9306 | 0.9241 |
| | narrow_brown_spot_HE_I917 | 0.9268 | 0.8539 | |
| | accuracy | 0.8868 | 0.8868 | 0.8868 |
| HE-processed Image (V channel) | macro avg | 0.8918 | 0.8879 | 0.8882 |
| | weighted avg | 0.8895 | 0.8868 | 0.8865 |
| | bacterial_leaf_blight_HE9V33 | 1.0000 | 0.9865 | |
| | brown_spot_HE_V | 0.6842 | 0.8228 | 0.7471 |
| | healthy_HE_V | 0.7545 | 0.9540 | 0.8426 |
| | leaf_blast_HE_V | 0.8222 | 0.4405 | 0.5736 |
| | leaf_scald_HE_V | 0.9531 | 0.8472 | 0.8971 |
| | narrow_brown_spot_HE_AS523 | 0.9146 | 0.8824 | |
| CS-processed Image (0.5) | accuracy | 0.8260 | 0.8260 | 0.8260 |
| | macro avg | 0.8400 | 0.8299 | 0.8216 |
| | weighted avg | 0.8351 | 0.8260 | 0.8165 |
| | bacterial_leaf_blight_CS9853 | 0.9178 | 0.9504 | |
| | brown_spot_CS | 0.8140 | 0.8861 | 0.8485 |
| | healthy_CS | 0.9875 | 0.9080 | 0.9461 |
| | leaf_blast_CS | 0.8846 | 0.8214 | 0.8519 |
| | leaf_scald_CS | 0.9459 | 0.9722 | 0.9589 |
| CS- processed Image (2) | narrow_brown_spot_CS9011 | 1.0000 | 0.9480 | |
| | accuracy | 0.9161 | 0.9161 | 0.9161 |
| | macro avg | 0.9197 | 0.9176 | 0.9173 |
| | weighted avg | 0.9192 | 0.9161 | 0.9162 |
| | bacterial_leaf_blight_CS0000 | 1.0000 | 1.0000 | |
| | brown_spot_CS2 | 0.8289 | 0.7975 | 0.8129 |
| | healthy_CS2 | 0.9762 | 0.9425 | 0.9591 |
| | leaf_blast_CS2 | 0.8235 | 0.8333 | 0.8284 |

overall accuracy. The accuracy of both CS1 and CS2 is almost identical at approximately 91%-92%. In contrast, the HE models display the lowest overall accuracy at 82.6%, and 88.68% indicating that the preprocessing steps of HE and CS do not noticeably enhance the ability to differentiate between diseased and healthy leaves.

V. CONCLUSION AND FUTURE WORK

The difference between image quality metrics like PSNR, MSE, and SSIM, and the accuracy in classifying images can be attributed to the fundamental variations in what these metrics measure. While PSNR, NRMSE, and SSIM focus on quantifying visual quality and fidelity based on mathematical calculations; image classification accuracy is a subjective measure that assesses the ability of a classifier to accurately categorize images. The discrepancy arises from the fact that high PSNR, low NRMSE, and high SSIM values indicate good image quality in terms of noise, sharpness, and structural similarity, but they do not directly translate to improved performance in image classification tasks. Factors such as classification algorithms' complexity and model robustness to noise and distortions play key roles in determining classification accuracy which may not always align with traditional image quality metrics. Therefore high image quality metrics indicate visual fidelity but do not guarantee optimal performance in image classification due to distinct evaluation criteria nature along with complexities involved both in processing images and development of clasification algorithms .

Based on the findings from the five models (original, histogram equalization in L channel, histogram equalization in V channel, contrast stretching with a power of 0.5, and contrast stretching with a power of 2), applying CS2 for detecting bacterial leaf blight is slightly more efficient than using the original image. Hence, there are certain diseases that preprocessing technique should be applied and not applicable to all classes because still original image shows higher accuracy compared to the one with preprocessing applied. While preprocessing techniques such as histogram equalization and contrast stretching can be used to enhance image quality, their application may not be necessary if the initial image dataset is already of sufficient quality. In such cases, applying these preprocessing methods could potentially degrade the image quality and lead to reduced classification accuracy. However, if the image dataset is poor, employing preprocessing techniques can be beneficial in improving the image quality and subsequently enhancing the performance of rice leaf disease detection.

Future works could involve exploring the implementation of these findings in other CNN models to assess how different architectures may impact the relationship between image quality metrics and classification accuracy. Additionally, experimenting with alternative preprocessing techniques beyond histogram equalization and contrast stretching, such as edge detection or image segmentation, could provide further insights into the interplay between image enhancement and classification performance. Additionally, incorporating validated datasets from different organisms/tissues requiring improved

image quality will broaden the platform's applicability. Furthermore, transitioning from a web application to a mobile application could open up new avenues for real-time image processing and classification, catering to a broader user base and enhancing the accessibility and usability of the system.

REFERENCES

- [1] A. Inocencio and E. Ponce. [Online]. Available: <http://books.irri.org/2017-March-Rice-Report-Lessons-from-the-past-3-decades.pdf>
- [2] F. Bordey, C. Launio, J. Beltran, A. Litonjua, R. Manalili, A. Mataia, and P. Moya, "Game changer: Is ph rice ready to compete at least regionally," *Rice Science for Decision-Makers*, vol. 6, no. 1, 2015.
- [3] Aug 2023. [Online]. Available: [invalid URL removed]
- [4] S. Savary, A. Ficke, J.-N. Aubertot, and C. Hollier, "Crop losses due to diseases and their implications for global food production losses and food security," *Food Security*, vol. 4, no. 4, p. 519–537, Jul 2012.
- [5] S. Savary, L. Willocquet, S. J. Pethybridge, P. Esker, N. McRoberts, and A. Nelson, "The global burden of pathogens and pests on major food crops," *Nature Ecology Evolution*, vol. 3, no. 3, p. 430–439, Feb 2019.
- [6] V. Visaya, "Rice blast disease hits farms in cagayan valley," Feb 2022. [Online]. Available: <https://newsinfo.inquirer.net/1553556/rice-blast-disease-hits-farmsin-cagayan-valley>
- [7] K. Simkhada and R. Thapa, "Rice blast, a major threat to the rice production and its various management techniques," *Turkish Journal of Agriculture - Food Science and Technology*, vol. 10, no. 2, p. 147–157, Mar 2022.
- [8] R. Li, S. Chen, H. Matsumoto, M. Gouda, Y. Gafforov, M. Wang, and Y. Liu, "Predicting rice diseases using advanced technologies at different scales: Present status and future perspectives," *aBIOTECH*, vol. 4, no. 4, p. 359–371, Nov 2023.
- [9] K. Li, X. Li, B. Liu, C. Ge, Y. Zhang, and L. Chen, "Diagnosis and application of rice diseases based on deep learning," *PeerJ Computer Science*, vol. 9, Jun 2023.
- [10] S. D. Fabiyi, H. Vu, C. Tachtatzis, P. Murray, D. Harle, T. K. Dao, I. Andonovic, J. Ren, and S. Marshall, "Varietal classification of rice seeds using rgb and hyperspectral images," *IEEE Access*, vol. 8, p. 22493–22505, 2020.
- [11] P. Song, P. Song, H. Yang, T. Yang, J. Xu, and K. Wang, "Detection of rice seed vigor by low-field nuclear magnetic resonance," *International Journal of Agricultural and Biological Engineering*, vol. 11, no. 6, p. 195–200, 2018.
- [12] D. Kusumaningrum, H. Lee, S. Lohumi, C. Mo, M. S. Kim, and B. Cho, "Non-destructive technique for determining the viability of soybean (glycine max) seeds using ft-nir spectroscopy," *Journal of the Science of Food and Agriculture*, vol. 98, no. 5, p. 1734–1742, Oct 2017.
- [13] D. Costa, J. Kodde, and S. Groot, "Chlorophyll fluorescence and x-ray analyses to characterise and improve paddy rice seed quality," *Seed Science and Technology*, vol. 42, no. 3, p. 449–453, Dec 2014.
- [14] P. Ramakrishna, "Grain scans: Fast x-ray fluorescence microscopy for high-throughput elemental mapping of rice seeds," *Plant Physiology*, vol. 191, no. 3, p. 1465–1467, Dec 2022.
- [15] A. K. Singh, B. Ganapathysubramanian, S. Sarkar, and A. Singh, "Deep learning for plant stress phenotyping: Trends and future perspectives," *Trends in Plant Science*, vol. 23, no. 10, p. 883–898, Oct 2018.
- [16] A.-K. Mahlein, M. Kuska, J. Behmann, G. Polder, and A. Walter, "Hyperspectral sensors and imaging technologies in phytopathology: State of the art," *Annual Review of Phytopathology*, vol. 56, no. 1, p. 535–558, Aug 2018.
- [17] H. Sun, S. Li, M. Li, H. Liu, L. Qiao, and Y. Zhang, "Research progress of image sensing and deep learning in agriculture," *Trans. Chin. Soc. Agric. Mach.*, vol. 51, no. 5, pp. 1–17, 2020.
- [18] H. T. Nguyen, Q. T. Quach, C. L. Tran, and H. H. Luong, "Deep learning architectures extended from transfer learning for classification of rice leaf diseases," *Advances and Trends in Artificial Intelligence. Theory and Practices in Artificial Intelligence*, p. 785–796, 2022.
- [19] M. Gill, R. Anderson, H. Hu, M. Bennamoun, J. Petereit, B. Valliyodan, H. T. Nguyen, J. Batley, P. E. Bayer, and D. Edwards, "Machine learning models outperform deep learning models, provide interpretation and facilitate feature selection for soybean trait prediction," *BMC Plant Biology*, vol. 22, no. 1, Apr 2022.
- [20] M. M. Hasan, A. F. Uddin, M. R. Akhond, M. J. Uddin, M. A. Hossain, and M. A. Hossain, "Machine learning and image processing techniques for rice disease detection: A critical analysis," *International Journal of Plant Biology*, vol. 14, no. 4, p. 1190–1207, Dec 2023.
- [21] S. Sengupta, A. Dutta, S. A. Abdelmohsen, H. A. Alyousef, and M. Rahimi-Gorji, "Development of a rice plant disease classification model in big data environment," *Bioengineering*, vol. 9, no. 12, p. 758, Dec 2022.
- [22] G. K. Udayananda, C. Shyalika, and P. P. Kumara, "Rice plant disease diagnosing using machine learning techniques: A comprehensive review," *SN Applied Sciences*, vol. 4, no. 11, Oct 2022.
- [23] V. Meshram, K. Patil, V. Meshram, D. Hanchate, and S. Ramteke, "Machine learning in agriculture domain: A state-of-art survey," *Artificial Intelligence in the Life Sciences*, vol. 1, p. 100010, 2021. [Online]. Available: <https://www.sciencedirect.com/science/article/pii/S2667318521000106>
- [24] S. Aggarwal, M. Suchithra, N. Chandramouli, M. Sarada, A. Verma, D. Vetrithangam, B. Pant, and B. Ambachew Adugna, "Rice disease detection using artificial intelligence and machine learning techniques to improvise agro-business," *Scientific Programming*, vol. 2022, p. 1–13, Jun 2022.
- [25] P. K. Sethy, N. K. Barpanda, A. K. Rath, and S. K. Behera, "Deep feature based rice leaf disease identification using support vector machine," *Computers and Electronics in Agriculture*, vol. 175, p. 105527, Aug 2020.
- [26] S. R. Shah, S. Qadri, H. Bibi, S. M. Shah, M. I. Sharif, and F. Marinello, "Comparing inception v3, vgg 16, vgg 19, cnn, and resnet 50: A case study on early detection of a rice disease," *Agronomy*, vol. 13, no. 6, p. 1633, Jun 2023.
- [27] P. Pukkela and S. Borra, "Machine learning based plant leaf disease detection and severity assessment techniques: State-of-the-art," *Lecture Notes in Computational Vision and Biomechanics*, p. 199–226, Nov 2017.
- [28] P. L. Chithra and P. Bhavani, "A study on various image processing techniques," *International Journal of Emerging Technology and Innovative Engineering*, vol. 5, no. 5, May 2019.
- [29] N. Petrellis, "A review of image processing techniques common in human and plant disease diagnosis," *Symmetry*, vol. 10, no. 7, p. 270, Jul 2018.
- [30] S. Sood, H. Singh, and M. Malarvel, "Image quality enhancement for wheat rust diseased images using histogram equalization technique," *2021 5th International Conference on Computing Methodologies and Communication (ICCMC)*, Apr 2021.
- [31] O. S. Temiatse, S. Misra, C. Dhawale, R. Ahuja, and V. Matthews, "Image enhancement of lemon grasses using image processing techniques (histogram equalization)," *Data Science and Analytics*, p. 298–308, 2018.
- [32] Deepa, "A pre processing approach for accurate identification of plant diseases in leaves," *2018 International Conference on Electrical, Electronics, Communication, Computer, and Optimization Techniques (ICEECOT)*, Dec 2018.
- [33] S. Jasrotia, J. Yadav, N. Rajpal, M. Arora, and J. Chaudhary, "Convolutional neural network based maize plant disease identification," *Procedia Computer Science*, vol. 218, p. 1712–1721, 2023.
- [34] D. S. Guru, P. B. Mallikarjuna, and S. Manjunath, "Segmentation and classification of tobacco seedling diseases," *Proceedings of the Fourth Annual ACM Bangalore Conference*, Mar 2011.
- [35] K. Padmavathi and K. Thangadurai, "Implementation of rgb and grayscale images in plant leaves disease detection – comparative study," *Indian Journal of Science and Technology*, vol. 9, no. 6, Feb 2016.
- [36] R. cua nguoi ta, "rice disease dataset," <https://universe.roboflow.com/rice-cua-nguoi-ta/rice-disease-d2wz6>, sep 2023. [Online]. Available: <https://universe.roboflow.com/rice-cua-nguoi-ta/rice-disease-d2wz6>
- [37] W. Zhihong and X. Xiaohong, "Study on histogram equalization," *2011 2nd International Symposium on Intelligence Information Processing and Trusted Computing*, Oct 2011.
- [38] S. S. Negi and Y. S. Bhandari, "A hybrid approach to image enhancement using contrast stretching on image sharpening and the analysis of various cases arising using histogram," *International Conference on Recent Advances and Innovations in Engineering (ICRAIE-2014)*, May 2014.
- [39] C. Shorten and T. M. Khoshgoftaar, "A survey on image data augmentation for deep learning," *Journal of Big Data*, vol. 6, no. 1, Jul 2019.
- [40] M. K. D. Mojár and V. R. Madrid, 2021.
- [41] M. Nadipally, "Optimization of methods for image-texture segmentation using ant colony optimization," *Intelligent Data Analysis for Biomedical Applications*, p. 21–47, 2019.
- [42] "skimage 0.23.2 documentation." [Online]. Available: <https://scikit-image.org/docs/stable/api/skimage.metrics.html>
- [43] D. R. Bull and F. Zhang, "Chapter 4 - digital picture formats and representations," in *Intelligent Image and Video Compression*

- (Second Edition), second edition ed., D. R. Bull and F. Zhang, Eds. Oxford: Academic Press, 2021, pp. 107–142. [Online]. Available: <https://www.sciencedirect.com/science/article/pii/B978012820353800013X>
- [44] Computer-Nerd, “Nrmse (normalized root mean squared error),” Mar 2023. [Online]. Available: <https://computer-nerd-zettelkasten.tistory.com/entry/NRMSE-Normalized-Root-Mean-Squared-Error>
- [45] J. Pekinski, G. Mikolajczak, and J. P. Kowalski, “Elimination of matching digital images to identify objective measures of quality,” 2014 Tenth International Conference on Intelligent Information Hiding and Multimedia Signal Processing, Aug 2014.
- [46] G. Zhai and X. Min, “Perceptual image quality assessment: A survey,” *Science China Information Sciences*, vol. 63, no. 11, Apr 2020.
- [47] I. A. Sabilla, M. Meirisdiana, D. Sunaryono, and M. Husni, “Best ratio size of image in steganography using portable document format with evaluation rmse, psnr, and ssim,” 2021 4th International Conference of Computer and Informatics Engineering (IC2IE), 09 2021.
- [48] A. Bovik, Z. Wang, and H. Sheikh, “Structural similarity based image quality assessment,” *Signal Processing and Communications*, p. 225–241, Nov 2005.
- [49] X. Ying, “An overview of overfitting and its solutions,” *Journal of Physics: Conference Series*, vol. 1168, p. 022022, Feb 2019.
- [50] Bharathi, “Latest guide on confusion matrix for multi-class classification,” Feb 2024. [Online]. Available: <https://www.analyticsvidhya.com/blog/2021/06/confusion-matrix-for-multi-class-classification/>